EuroIntervention
2025;21:e820-e823
published online e-edition July 2025
DOI: 10.4244/EIJ-D-25-00025

Validation of the pullback pressure gradient in resting conditions

Koshiro Sakai[1,2,3], MD, PhD; Jeroen Sonck[1], MD, PhD; Takuya Mizukami[1,4,5], MD, PhD; Hitoshi Matsuo[5], MD, PhD; Brian Ko[6], MD, PhD; Divaka Perera[7], FRCP, MD; Hirohiko Ando[8], MD, PhD; Simone Biscaglia[9], MD, PhD; Fernando Rivero[10], MD, PhD; Antonio Maria Leone[11,12], MD, PhD; Liyew Desta[13], MD, PhD; Javier Escaned[14], MD, PhD; Masafumi Nakayama[15], MD, PhD; Daniel Munhoz[1], MD, PhD; Tatyana Storozhenko[1,16], MD; Hirofumi Ohashi[8], MD, PhD; Gianluca Campo[9], MD, PhD; Tetsuya Amano[8], MD, PhD; Toshiro Shinke[2], MD, PhD; Ziad Ali[3], MD, DPhil; Bernard De Bruyne[1,17], MD, PhD; Nils P. Johnson[18], MD, MS; Carlos Collet[1]*, MD, PhD; Allen Jeremias[3], MD, MSc

Corresponding author: Cardiovascular Center, AZORG, Moorselbaan 164, 9300, Aalst, Belgium. E-mail: carloscollet@gmail.com

This paper also includes supplementary data published online at: https://eurointervention.pcronline.com/doi/10.4244/EIJ-D-25-00025

The pullback pressure gradient (PPG) is a novel metric that quantifies coronary artery disease (CAD) patterns as focal or diffuse on a scale from 0 (diffuse) to 1 (focal)[1]. PPG predicts blood flow improvement after percutaneous coronary intervention (PCI): a high PPG (focal disease) is associated with greater flow improvement and angina relief, while a low PPG (diffuse disease) is linked to higher periprocedural complications[2,3]. Traditionally, PPG has been derived from fractional flow reserve (FFR) pullbacks. However, assessment using non-hyperaemic pressure ratios (NHPR) can shorten procedure time and eliminate the need for a hyperaemic agent. This study aimed to assess the agreement between resting and hyperaemic PPG.

This study was a prespecified subanalysis of the PPG Global Registry, a prospective, investigator-initiated, multicentre, international study (ClinicalTrials.gov: NCT04789317)[2]. Eligible patients had at least one haemodynamically significant lesion (FFR ≤0.80) scheduled for PCI, with those undergoing both resting and hyperaemic pressure pullbacks included **(Supplementary Figure 1)**. The pressure wire (PressureWire X [Abbott]) was placed in the distal coronary artery to measure resting distal coronary pressure/aortic pressure, resting full-cycle ratio (RFR), and FFR. Manual pullbacks were performed over 20-30 seconds. PPG was automatically calculated online using CoroFlow v3.5.1 software (Coroventis Research AB) **(Supplementary Figure 2)**. Resting PPG was calculated by the core lab (CoreAalst BV) using resting pressure pullbacks with the same algorithm. We classified functional patterns using the median hyperaemic PPG value of 0.62, derived from the entire PPG Global cohort, and applied the same threshold for resting PPG. Continuous variables were compared using Mann-Whitney U tests and categorical variables using chi-square tests. Pearson's correlation assessed associations, and Bland-Altman analysis, Passing-Bablok regression, and Cohen's Kappa evaluated agreement. The diagnostic performance of resting PPG was evaluated based on sensitivity, specificity, positive predictive value, and negative predictive value. Receiver operating characteristic analysis assessed the predictive capacity for optimal PCI outcomes (post-PCI FFR ≥0.88), with the area under the curve (AUC) comparisons performed using the DeLong method.

Between December 2020 and September 2023, 1,004 patients (1,057 vessels) were enrolled, of whom 88 patients (90 vessels) underwent both resting and hyperaemic pressure pullbacks. Patient and procedural characteristics are shown in **Supplementary Table 1** and **Supplementary Table 2**. The mean resting and hyperaemic PPG were 0.67±0.14 and 0.63±0.16 **(Figure 1A)**, respectively, with a mean difference of 0.04 (95% limits of agreement: –0.23 to 0.15) and a strong correlation **(Figure 1B, Figure 1C)**. Passing-Bablok regression showed systematic and proportional differences, with coefficient A at 0.13 (95% confidence interval [CI]: 0.05 to 0.22) and coefficient B at 0.86 (95% CI: 0.73 to 0.98). Correlation between resting and hyperaemic PPG among vessels with FFR in the grey zone (0.75 <FFR <0.80) is shown in **Supplementary Figure 3**. Resting and hyperaemic maximal pressure gradients correlated strongly, while correlation on

SUBMITTED ON 05/01/2025 - REVISION RECEIVED ON 1st 02/03/2025 / 2nd 05/04/2025 - ACCEPTED ON 07/04/2025

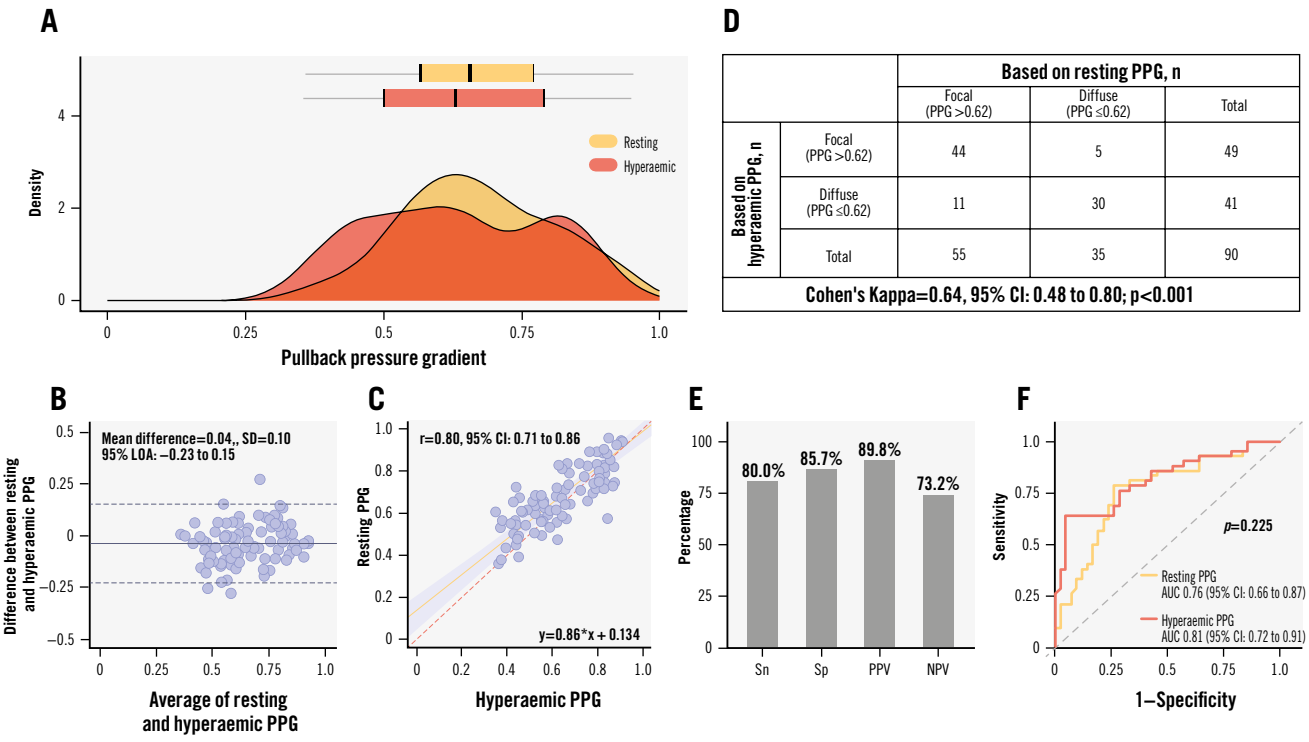

Figure 1. *Distribution, correlation, agreement, diagnostic performance, and predictive capacity for optimal PCI outcomes between resting and hyperaemic PPG. A) Distribution of resting and hyperaemic PPG. B) Bland-Altman analysis comparing resting and hyperaemic PPG. C) Correlation between resting and hyperaemic PPG. D) The Cohen's Kappa analysis demonstrated a substantial agreement in CAD pattern classification between resting and hyperaemic PPG. E) Diagnostic performance of resting PPG, including sensitivity (Sn), specificity (Sp), positive predictive value (PPV), and negative predictive value (NPV). F) Comparison of the predictive capacity of resting PPG (orange) and hyperaemic PPG (red) for achieving optimal PCI (post-PCI FFR >0.88). AUC: area under the curve; CAD: coronary artery disease; CI: confidence interval; LOA: limits of agreement; PCI: percutaneous coronary intervention; PPG: pullback pressure gradient; SD: standard deviation*

the disease extent was moderate **(Supplementary Figure 4)**. The concordance between resting and hyperaemic PPG was 82%, with substantial agreement in CAD pattern classification **(Figure 1D)**. Resting PPG showed good diagnostic performance **(Figure 1E)**. Agreement and diagnostic performance for different PPG cutoffs are shown in **Supplementary Figure 5**. A high resting PPG (>0.62) was associated with higher post-PCI FFR and RFR and correlated with delta FFR **(Supplementary Figure 6)**. The predictive capacity of resting PPG for optimal PCI (AUC=0.76) was similar to hyperaemic PPG **(Figure 1F)**. A comparison of predictive capacity stratified by vessel type is shown in **Supplementary Figure 7**.

This study demonstrated a strong correlation between resting and hyperaemic PPG and substantial agreement in CAD pattern classification, suggesting that resting PPG may serve as a practical alternative to hyperaemic PPG for assessing CAD patterns. Vessels with a higher resting PPG achieved greater flow improvement after PCI, with predictive accuracy comparable to hyperaemic PPG. The agreement between resting and hyperaemic PPG was approximately 80%, similar to the concordance observed between NHPR and FFR. Given its procedural simplicity, shorter duration, and comparable diagnostic performance, resting PPG presents a practical alternative to hyperaemic PPG for quantifying CAD patterns.

This study has several limitations. Potential selection bias may be present, and the predominance of left anterior descending artery lesions (83%) may limit generalisability. Additionally, the sample size was relatively small, and the study only included vessels with FFR ≤0.80. The optimal PPG cutoff remains undefined, and the study is underpowered to detect significant differences in predictive capacity. Therefore, these findings should be interpreted as hypothesis-generating, warranting further validation in larger and more diverse cohorts.

In conclusion, resting PPG demonstrated a high level of agreement with hyperaemic PPG and was associated with improved PCI outcomes, with vessels exhibiting a high resting PPG achieving greater post-PCI FFR and RFR than those with a low resting PPG.

Authors' affiliations

1. Cardiovascular Center Aalst, OLV Clinic, Aalst, Belgium; 2. Department of Medicine, Division of Cardiology, Showa University School of Medicine, Tokyo, Japan; 3. Department of Cardiology, St Francis Hospital and

Heart Center, Roslyn, NY, USA; 4. Division of Clinical Pharmacology, Department of Pharmacology, Showa University, Tokyo, Japan; 5. Department of Cardiovascular Medicine, Gifu Heart Center, Gifu, Japan; 6. Monash Cardiovascular Research Centre, Monash University and Monash Heart, Monash Health, Clayton, VIC, Australia; 7. School of Cardiovascular Medicine and Sciences, St Thomas' Hospital Campus, King's College London, London, United Kingdom; 8. Department of Cardiology, Aichi Medical University, Aichi, Japan; 9. Cardiology Unit, Azienda Ospedaliera Universitaria di Ferrara, Ferrara, Italy; 10. Cardiac Department, Hospital Universitario de La Princesa, IIS-IP, Madrid, Spain; 11. Department of Cardiovascular and Pneumological Sciences, Catholic University of the Sacred Heart, Rome, Italy; 12. Center of Excellence in Cardiovascular Sciences, Ospedale Isola Tiberina - Gemelli Isola, Rome, Italy; 13. Department of Cardiology, Karolinska University Hospital, Solna, Sweden; 14. Instituto de Investigacion Sanitaria del Hospital Clinico San Carlos and Complutense University, Madrid, Spain; 15. Department of Cardiology, Tokyo D Tower Hospital, Tokyo, Japan; 16. Department of Prevention and Treatment of Emergency Conditions, L.T. Malaya Therapy National Institute NAMSU, Kharkiv, Ukraine; 17. Department of Cardiology, University Hospital of Lausanne, Lausanne, Switzerland; 18. Division of Cardiology, Department of Medicine, Weatherhead PET Center, McGovern Medical School at UTHealth and Memorial Hermann Hospital, Houston, TX, USA

Funding

The study was sponsored by the Cardiac Research Institute Aalst with a research grant from Abbott Vascular.

Conflict of interest statement

T. Mizukami reports receiving research grants from Boston Scientific; and speaker fees from Abbott, CathWorks, and Boston Scientific. H. Matsuo has received consulting fees from Kaneka and Zeon; and speaker fees from Abbott, Boston Scientific, Philips, and Amgen. B. Ko has received consulting fees from Canon Medical, Abbott, and Medtronic. D. Perera has received research grant support from Abbott, HeartFlow, and Philips. S. Biscaglia received research grants provided by Sahajanand Medical Technologies, Medis Medical Imaging Systems, Eukon S.r.l., Siemens Healthineers, GE HealthCare, and Insight Lifetech. A.M. Leone reports receiving consultancy fees from Abbott; and honoraria for sponsored symposiums from Abbott, Medtronic, and Abiomed. J. Escaned is supported by the Intensification of Research Activity project INT22/00088 from Spanish Instituto de Salud Carlos III; and received speaker and advisory board member fees from Abbott and Philips. G. Campo reported receiving grants from Sahajanand Medical Technologies, GE HealthCare, Siemens Healthineers, Insight Lifetech, Abbott, and Amgen outside the submitted work. T. Amano reports receiving lecture fees from Astellas Pharma, AstraZeneca, Bayer, Daiichi Sankyo, and Bristol-Myers Squibb. T. Shinke received personal fees and research grants from Abbott. Z. Ali reports institutional grant support from Abbott, Abiomed, Acist, Amgen, Boston Scientific, CathWorks, Canon, Conavi, HeartFlow, Inari, Medtronic, National Institute of Health, Nipro, Opsens Medical, Medis Medical Imaging, Philips, Shockwave Medical, Siemens Healthineers, SpectraWAVE, and Teleflex; consulting fees from Abiomed, AstraZeneca, Boston Scientific, CathWorks, Opsens, Philips, Shockwave Medical; and equity in Elucid, Lifelink, SpectraWAVE, Shockwave Medical, and VitalConnect. B. De Bruyne reports receiving consultancy fees from Boston Scientific and Abbott; and research grants from Coroventis Research, Pie Medical Imaging, CathWorks, Boston Scientific, Siemens Healthineers, HeartFlow, and Abbott. N.P. Johnson received internal funding from the Weatherhead PET Center for Preventing and Reversing Atherosclerosis; has received significant institutional research support from St. Jude Medical (CONTRAST, NCT02184117) and Philips Volcano Corporation (DEFINE-FLOW, NCT02328820) for other studies using intracoronary pressure and flow sensors; has an institutional licensing agreement with Boston Scientific for the smart-minimum FFR algorithm (now commercialised under 510(k) K191008); and has patents pending on diagnostic methods for quantifying aortic stenosis and TAVI physiology, and on methods to correct pressure tracings from fluid-filled catheters. C. Collet reports receiving research grants from Biosensors, Coroventis Research, Medis Medical Imaging, Pie Medical Imaging, CathWorks, Boston Scientific, Siemens Healthineers, HeartFlow, and Abbott; and consultancy fees from HeartFlow, Opsens, Abbott, and Philips/Volcano. A. Jeremias has received consulting fees from Canon, Artrya Medical, and Boston Scientific. The other authors have no conflicts of interest to declare.

References

1. Collet C, Sonck J, Vandeloo B, Mizukami T, Roosens B, Lochy S, Argacha JF, Schoors D, Colaiori I, Di Gioia G, Kodeboina M, Suzuki H, Van 't Veer M, Bartunek J, Barbato E, Cosyns B, De Bruyne B. Measurement of Hyperemic Pullback Pressure Gradients to Characterize Patterns of Coronary Atherosclerosis. *J Am Coll Cardiol.* 2019;74:1772-84.

2. Collet C, Munhoz D, Mizukami T, Sonck J, Matsuo H, Shinke T, Ando H, Ko B, Biscaglia S, Rivero F, Engstrøm T, Arslani K, Leone AM, van Nunen LX, Fearon WF, Christiansen EH, Fournier S, Desta L, Yong A, Adjedj J, Escaned J, Nakayama M, Eftekhari A, Zimmermann FM, Sakai K, Storozhenko T, da Costa BR, Campo G, West NEJ, De Potter T, Heggermont W, Buytaert D, Bartunek J, Berry C, Collison D, Johnson T, Amano T, Perera D, Jeremias A, Ali Z, Pijls NHJ, De Bruyne B, Johnson NP. Influence of Pathophysiologic Patterns of Coronary Artery Disease on Immediate Percutaneous Coronary Intervention Outcomes. *Circulation.* 2024;150:586-97.

3. Collet C, Collison D, Mizukami T, McCartney P, Sonck J, Ford T, Munhoz D, Berry C, De Bruyne B, Oldroyd K. Differential Improvement in Angina and Health-Related Quality of Life After PCI in Focal and Diffuse Coronary Artery Disease. *JACC Cardiovasc Interv.* 2022;15:2506-18.

Supplementary data

Supplementary Table 1. Baseline clinical characteristics.
Supplementary Table 2. Angiographic and physiological demographics.
Supplementary Figure 1. Study flowchart.
Supplementary Figure 2. PPG calculation.
Supplementary Figure 3. Correlation between resting and hyperaemic PPG among vessels with FFR in the grey zone.

Supplementary Figure 4. Correlation of maximum pressure gradients normalised by vessel gradient and percentage diseased length at rest and during hyperaemia.

Supplementary Figure 5. Agreement and diagnostic performance using different resting PPG cutoffs.

Supplementary Figure 6. Differences in post-PCI FFR and RFR between focal and diffuse CAD, and correlation of resting PPG with functional improvement.

Supplementary Figure 7. Predictive capacity of PPG for optimal PCI results, stratified by vessel type.

The supplementary data are published online at: https://eurointervention.pcronline.com/doi/10.4244/EIJ-D-25-00025

Supplementary data

Supplementary Table 1. Baseline clinical characteristics.

Variables	Overall
Number of patients, n	88
Age, years (mean ± SD)	68.2 ± 9.8
Male, n (%)	66 (75.0)
BMI, kg/m^2 (mean ± SD)	27.3 ± 4.8
Dyslipidemia, n (%)	61 (69.3)
Hypertension, n (%)	59 (67.0)
Diabetes mellitus, n (%)	21 (23.9)
Smoking, n (%)	15 (17.0)
Prior PCI, n (%)	5 (5.7)
Prior MI, n (%)	10 (11.4)
Creatinine clearance, ml/min (mean ± SD)	73.1 ± 25.8
LVEF, % (mean ± SD)	61.5 ± 8.3
Clinical presentation, n (%)	
Asymptomatic, n (%)	11 (12.5)
Silent ischaemia*, n (%)	5 (5.7)
CCS I, n (%)	42 (47.7)
CCS II, n (%)	22 (25.0)
CCS III, n (%)	5 (5.7)
CCS IV, n (%)	0 (0)
Unstable angina, n (%)	3 (3.4)

* Silent ischemia is defined as asymptomatic patients with a positive non-invasive test.
BMI body mass index. CCS Canadian Cardiovascular Society. LVEF left ventricular ejection fraction. MI myocardial infarction. PCI percutaneous coronary intervention. SD standard deviation.

Supplementary Table 2. Angiographic and physiological demographics.

Variables	Overall
Number of vessels, n	90
Vessels	
LAD, n (%)	75 (83.3)
LCx, n (%)	6 (6.7)
RCA, n (%)	9 (10.0)
With serial lesions*, n (%)	19 (21.1)
QCA analysis	
Minimum lumen diameter, mm (mean ± SD)	1.6 ± 0.54
Reference lumen diameter, mm (mean ± SD)	2.7 ± 0.6
Percent diameter stenosis, % (mean ± SD)	49.9 ± 15.9
Pre-PCI physiological analysis	
Resting Pd/Pa, (mean ± SD)	0.82 ± 0.13
RFR, (mean ± SD)	0.75 ± 0.16
FFR, (mean ± SD)	0.66 ± 0.11
Post-PCI physiological analysis	
Number of PCI, n (%)	84 (94.4)
Resting Pd/Pa, (mean ± SD)	0.94 ± 0.04
RFR, (mean ± SD)	0.91 ± 0.05
FFR, (mean ± SD)	0.87 ± 0.07

*Serial lesions were site-reported based on angiography alone.

FFR fractional flow reserve. LAD left anterior descending artery. LCx left circumflex artery. Pa aortic pressure. PCI percutaneous coronary intervention. Pd distal coronary pressure. QCA quantitative coronary angiography. RCA right coronary artery. RFR resting full-cycle ratio. SD standard deviation.

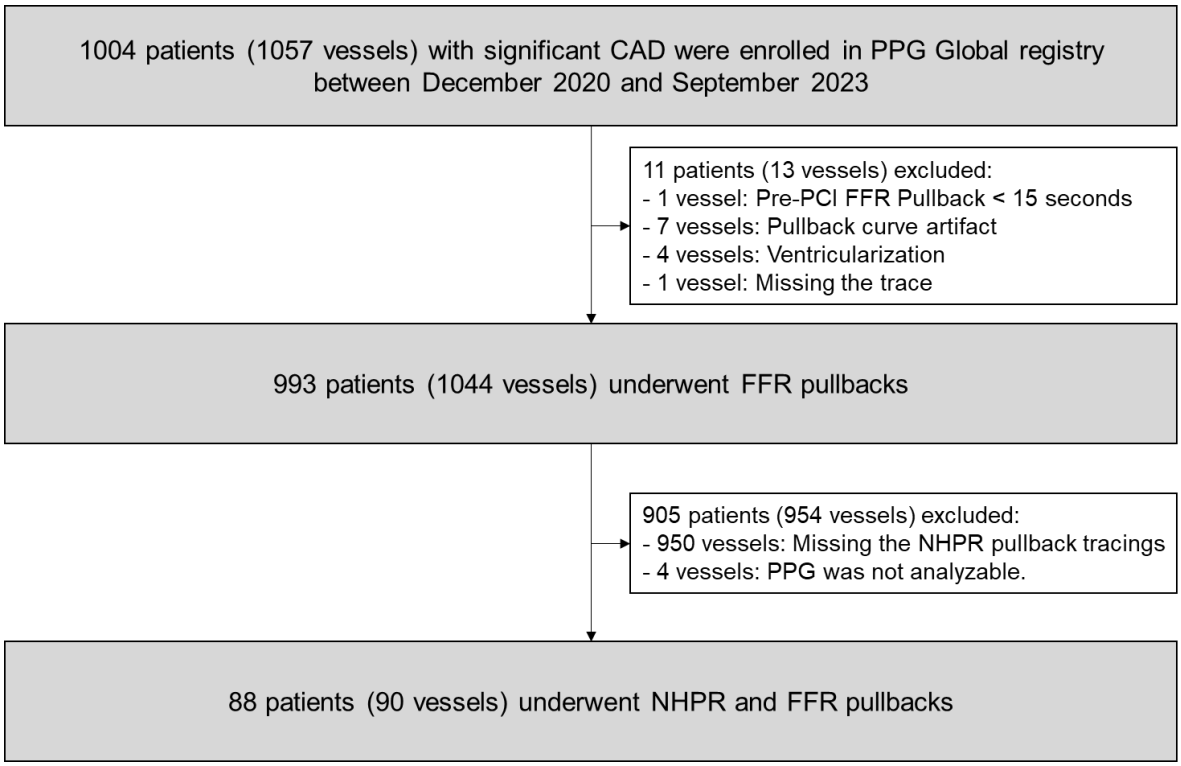

Supplementary Figure 1. Study flowchart.

CAD coronary artery disease. FFR fractional flow reserve. NHPR non-hyperemic pressure ratios. PCI percutaneous coronary intervention. PPG pullback pressure gradient.

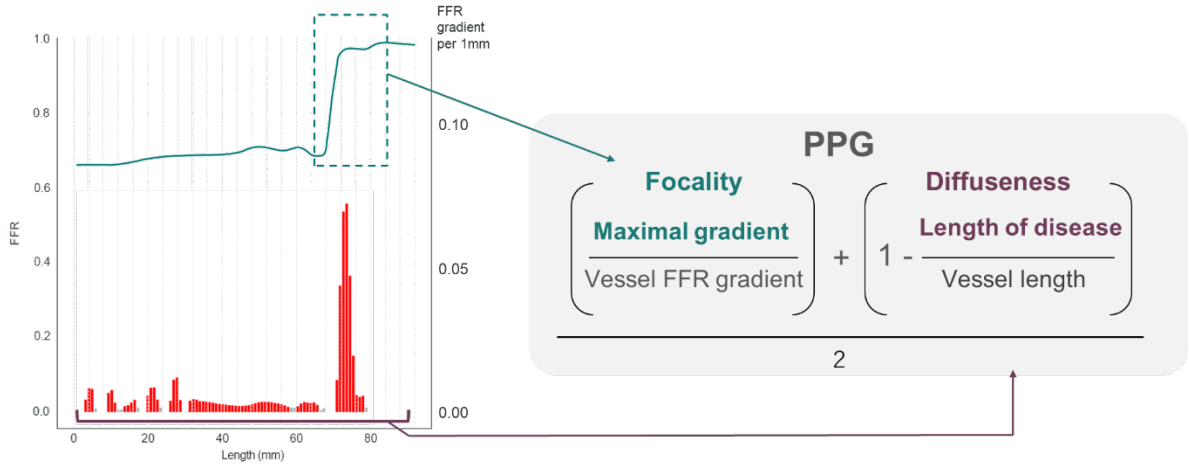

Supplementary Figure 2. PPG calculation.

PPG combines two parameters extracted from the FFR pullback curve: the maximal pressure gradient over 20% of the pullback during maximal hyperemia and the length of functional disease (PPG range: 0 [diffuse] to 1 [focal]).

FFR fractional flow reserve. PPG pullback pressure gradient.

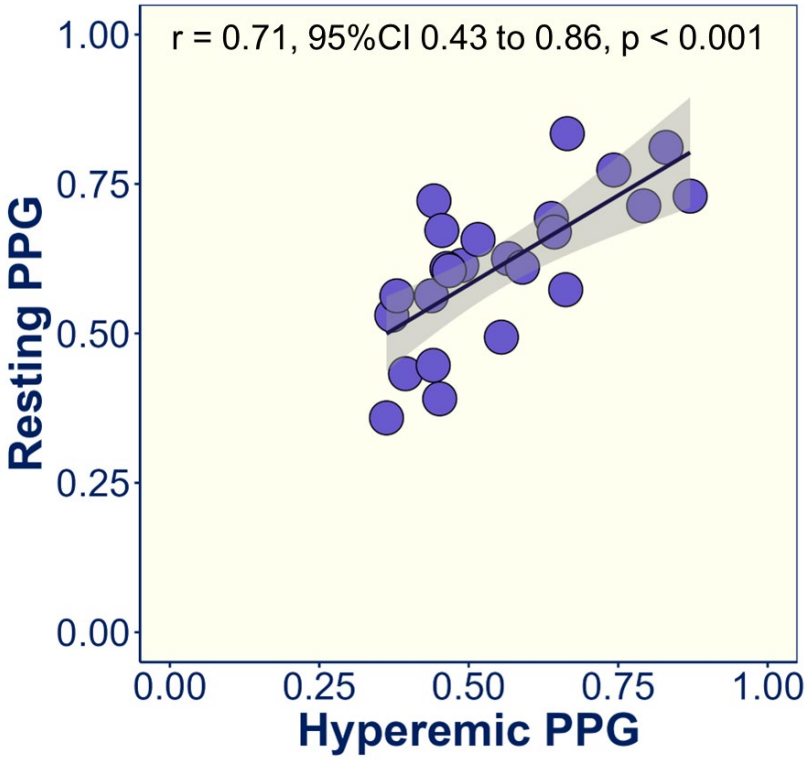

Supplementary Figure 3. Correlation between resting and hyperaemic PPG among vessels with FFR in the grey zone.

Vessels with FFR in the gray zone was defined as pre-PCI FFR between 0.75 and 0.80.

CI confidence interval. FFR fractional flow reserve. PCI percutaneous coronary intervention. PPG pullback pressure gradient.

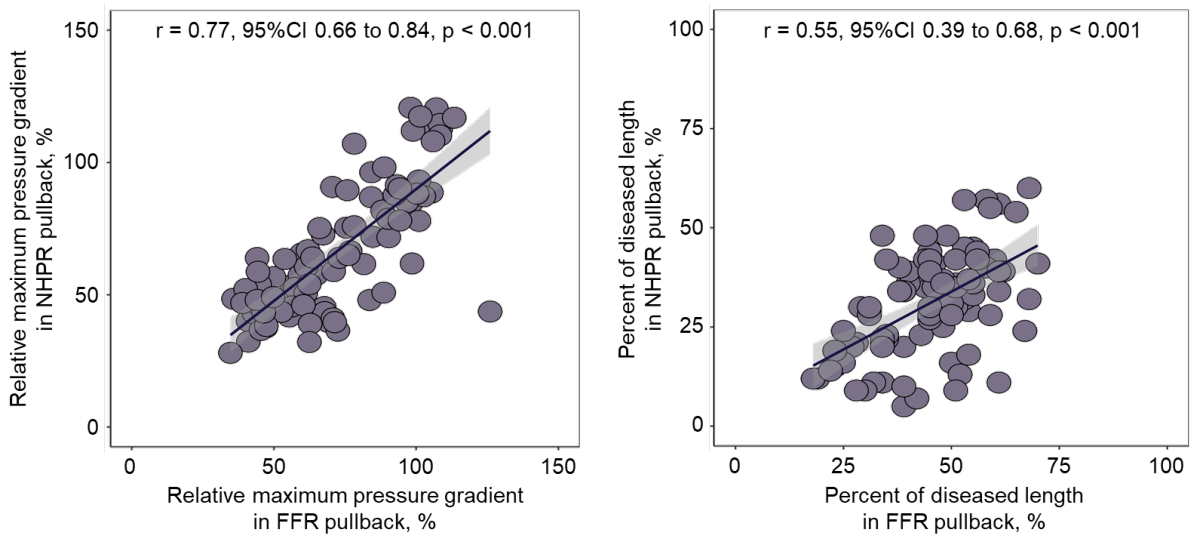

Supplementary Figure 4. Correlation of maximum pressure gradients normalised by vessel gradient and percentage diseased length at rest and during hyperaemia.

The left panel presents the correlation of relative maximum pressure gradient, and the right panel shows the correlation of percent diseased length.

CI confidence interval. FFR fractional flow reserve. NHPR non-hyperemic pressure ratios.

		Based on resting PPG, n		
		Focal (PPG > 0.50)	Diffuse (PPG ≤ 0.50)	Total
Based on hyperemic PPG, n	Focal (PPG > 0.50)	65	2	67
	Diffuse (PPG ≤ 0.50)	16	7	23
	Total	81	9	90
Cohen's Kappa = 0.34, 95%CI: 0.12 to 0.56				

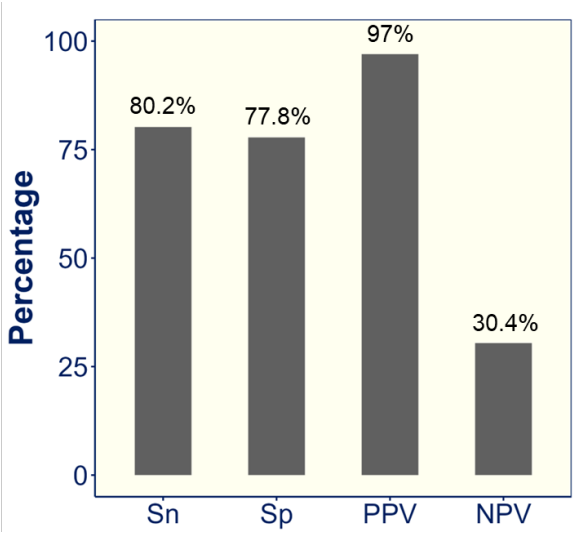

		Based on resting PPG, n		
		Focal (PPG > 0.66)	Diffuse (PPG ≤ 0.66)	Total
Based on hyperemic PPG, n	Focal (PPG > 0.62)	40	9	49
	Diffuse (PPG ≤ 0.62)	5	36	41
	Total	45	45	90
Cohen's Kappa = 0.69, 95%CI: 0.54 to 0.84				

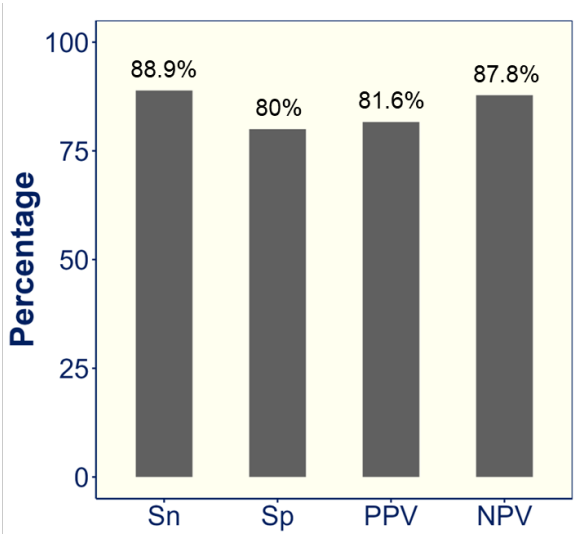

Supplementary Figure 5. Agreement and diagnostic performance using different resting PPG cutoffs.

The top panels show the agreement of functional CAD patterns (left) and diagnostic performance (right) using the same PPG cut-off of 0.50 for both resting and hyperemic conditions. The bottom panels show the agreement of functional CAD patterns (left) and diagnostic performance (right) using separate PPG cut-offs. The resting PPG cut-off of 0.66 was derived from the median value in the present cohort.

CAD coronary artery disease. CI confidence interval. NPV negative predictive value, Sn sensitivity, Sp specificity, PPG pullback pressure gradient, PPV positive predictive value.

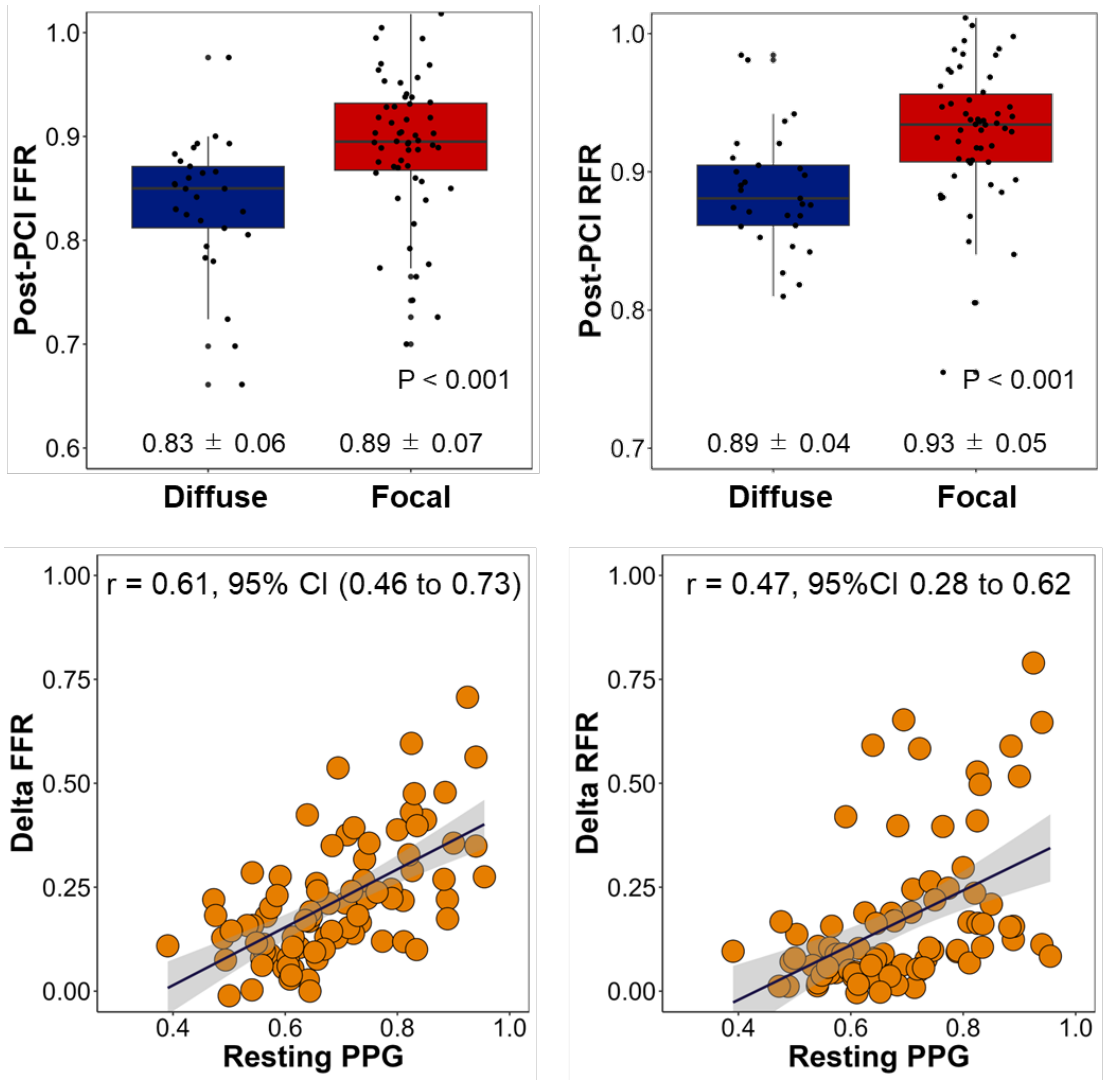

Supplementary Figure 6. Differences in post-PCI FFR and RFR between focal and diffuse CAD, and correlation of resting PPG with functional improvement.

The top panels compare post-PCI FFR (left) and RFR (right) between functional CAD patterns (focal in red, diffuse in blue) classified by resting PPG. The bottom panels illustrate the correlation of resting PPG with delta FFR (post-PCI FFR – pre-PCI FFR) on the left and delta RFR (post-PCI RFR – pre-PCI RFR) on the right.

CAD coronary artery disease. CI confidence interval. FFR fractional flow reserve. PCI percutaneous coronary intervention. PPG pullback pressure gradient. RFR resting full-cycle ratio.

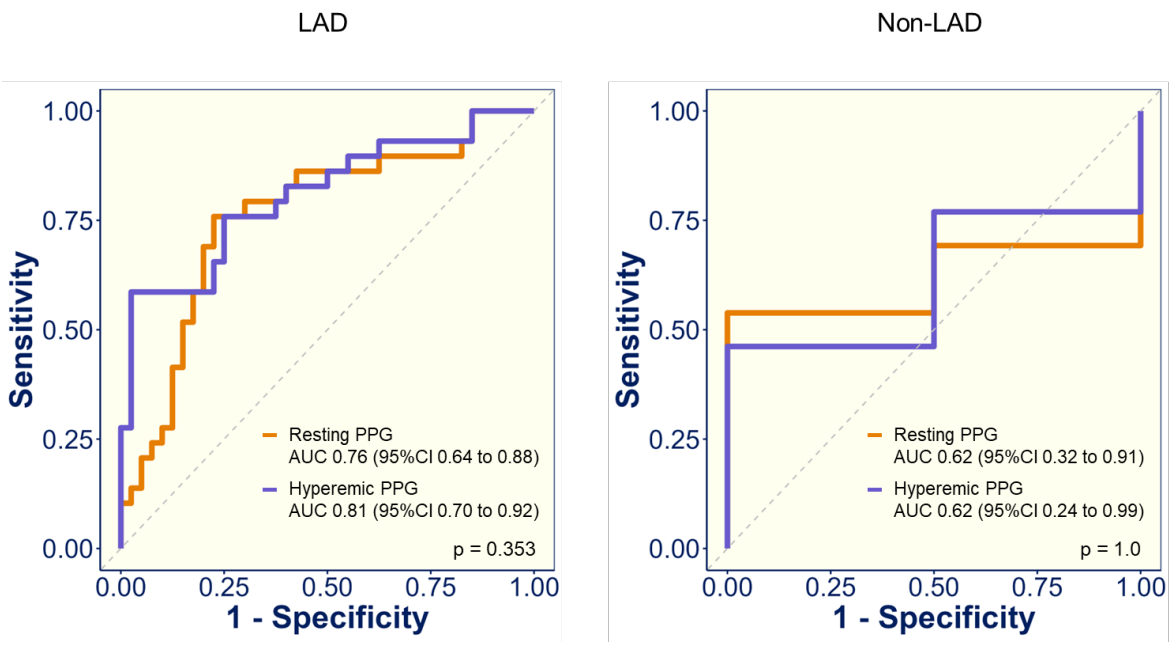

Supplementary Figure 7. Predictive capacity of PPG for optimal PCI results, stratified by vessel type.

Comparison of the predictive capacity of PPG for achieving a functionally optimal PCI outcome (post-PCI FFR ≥0.88) between resting PPG (orange) and hyperemic PPG (purple), stratified by vessel type: LAD (left) and non-LAD (right). Resting and hyperemic PPG demonstrate similar predictive capacity for optimal PCI outcomes.

AUC area under the curve. CI confidence interval. FFR fractional flow reserve. LAD left anterior descending artery. PCI percutaneous coronary intervention. PPG pullback pressure gradient.